Investigation of Gyroscopes Mechanical and Electronic Phase Drift with 2 μrad/√Hz Resolution and 12 μrad/K Accuracy

Leonardo Gaffuri Pagani[1], Luca Guerinoni[2], Luca Falorni[2], Patrick Fedeli[2], and Giacomo Langfelder[1]
Contact author email: leonardo.gaffuri@polimi.it
[1]Politecnico di Milano, Italy and [2]ST Microelectronics, Cornaredo (MI), Italy

***Abstract*— The work demonstrates a setup for the accurate calibration of the relative phase drift between sense modulated output and drive demodulation reference in MEMS gyroscopes. The system enables to operate the sensor inside a climatic chamber, with all the electronics outside, reaching 2 μrad/√Hz short-term resolution in relative phase measurements. After a one-time calibration of parasitic electrical couplings, the setup enables to measure the phase drift in temperature with a sub-5-μrad long-term stability. On average, measurements over four samples, swept vs temperature in 18 different operating conditions, deviate from modeling by 12 μrad/K only.**

Keywords — calibration, MEMS, gyroscopes, stability.

I. INTRODUCTION

Accurate calibration of the zero-rate-output vs temperature in amplitude-modulated (AM) gyroscopes represents a key step towards improved stability. This is ultimately determined by relative phase drifts $\Delta\phi_{DS}(T)$ between sense modulated signal (induced by the Coriolis force) and drive-loop demodulation reference, which brings quadrature into the output. As an example, a gyroscope with 1-dps residual quadrature (after compensation [1]) requires a *demodulation phase stability* within 1 mrad (about 10 μrad/K over the temperature consumer range) to ensure an overall 1-mdps *rate stability*. Such value could open the path to next-generation application of virtual-world and real-world inertial navigation.

In current integrated circuit implementations, a real-time measurement of $\Delta\phi_{DS}$ is not possible, but its online compensation vs temperature could be implemented if the errors $\Delta\phi_{DS}(T)$ were initially calibrated. Though few works introduced this issue [2-4], none of them ever (i) conceived a dedicated setup to measure the drift $\Delta\phi_{DS}(T)$, (ii) identified critical noise contributions for such measurements and (iii) experimentally isolated, from electronic couplings drifts, the mechanical drift induced by temperature changes of mode-split and quality factor. This work fulfills all these tasks, using as a test device the pitch axis of the triaxial, single-drive gyroscope shown in Fig. 1a. The device has frequencies in the 20 kHz range, split by about 500 Hz, with drive and sense quality factors in the range of 7000 and 700, respectively [5].

The reference model for the mechanical drift is shown by the simulations of modulus and phase of its sense mode, as a function of temperature, reported in Fig. 1b-c: for the sake of clarity, the drive mode frequency is only shown by dashed vertical lines. Every color curve corresponds to a different temperature point in the range 20°C to 90°C. The zoom highlights the value of the sense-mode transfer function phase excited at the drive frequency. When the temperature changes, both the frequency of the two modes and their quality factor change. Correspondingly, a change in the phase $\Delta\phi_{DS}(T)$ of the sense mode response to a Coriolis force (modulated at the drive frequency) can be observed, with a value in the order of 6 mrad, which grows up to more than 10 mrad when the entire consumer temperature range is taken into account.

The next section describes the methodology adopted to isolate this mechanical drift from drift of electronic couplings, and to optimize the resolution in relative phase noise measurements. Afterwards, experimental results and agreement with models will be presented when operating four different samples in, overall, 18 various operating conditions of drive amplitude, mode split and quadrature error value.

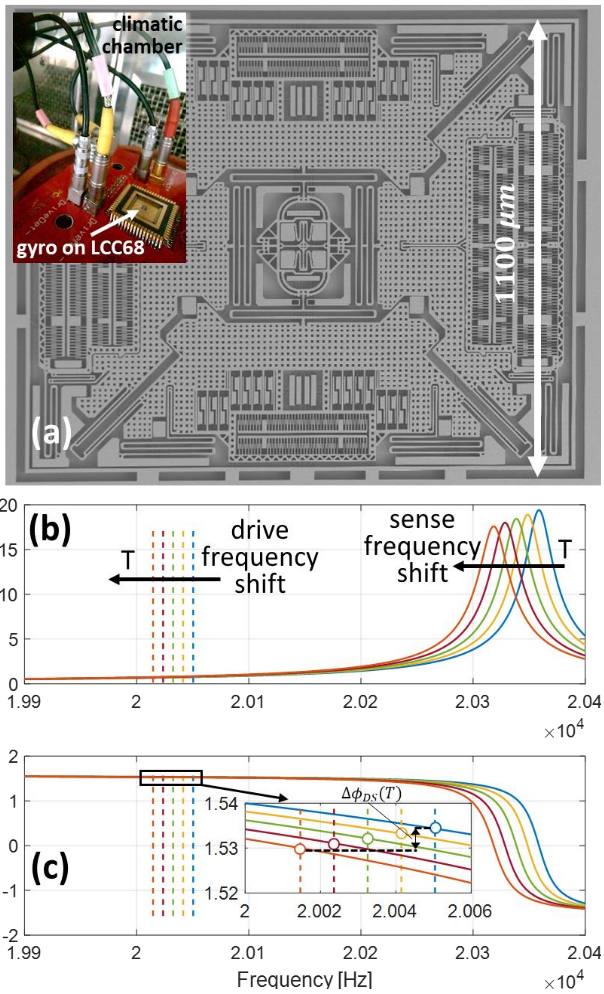

Fig. 1: top-view of the single-drive 3-axis gyroscope (a), whose pitch axis is studied vs T (see the inset) in this work. In mode-split operation (frequencies of 20 kHz, split of few 100 Hz) the sense transfer function (b-c) is excited by the drive mode with a phase $\Delta\phi_{DS}$ drifting by ~6 mrad under temperature changes (20°C to 90°C in the figure) due to changes vs T (TCf, [6]) in the mode split and in the sense quality factor (TCQ, [7]).

This work was partly supported under the European Union ENIAC project ArrowHead Tools, grant agreement n. 826452.

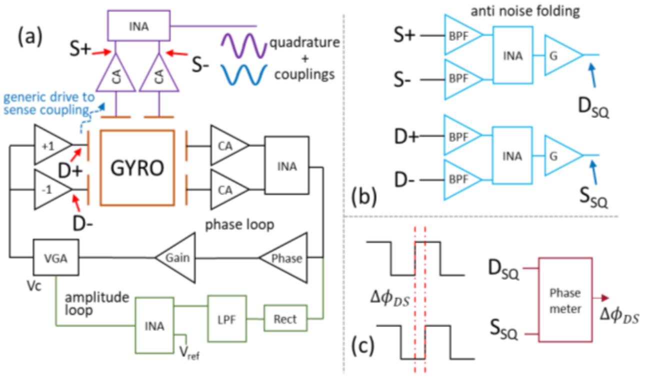

Fig. 2: block scheme of the developed circuit, including (a) the drive-mode phase loop (black), the amplitude controller (green) and the sense chain (purple). Differential signals at the drive and sense ports are (b) properly filtered (BPF) to avoid noise folding, amplified (cyan) and (c) sent to a phase meter (red). Note the indication of a generic coupling term, with its own phase, from the drive loop into the sense chain.

II. METHODOLOGY

The MEMS gyroscope is isolated from its sustaining and readout circuits using a separate ceramic carrier (see the inset of Fig. 1a), which is placed inside a climatic chamber. This somewhat limits the achievable noise resolution in relative phase measurements because parasitics of long cables amplify electronic noise of the drive-detection and sense-detection amplifying stages. Nevertheless, this is the only way:

(i) to allow calibration of the setup parasitics (in particular coupling drive signals into the sense chain) once for all tested MEMS. Indeed, when changing the MEMS to test in the proposed scenario, one just needs to change the carrier holding the device, leaving all cables and boards unmodified;

(ii) to bypass the contributions represented by drifts of such parasitic couplings. As the couplings (and their drifts due to drive-mode quality factor changes vs T) are always repeatable whatever the MEMS, they can be subtracted in the same way for all the measured devices.

Fig. 2a reports the developed circuit, including usual configurations [8, 9] for the drive oscillator and the sense chain (possible couplings of drive-loop signals into the sense path are also highlighted). Additionally, the differential signals at drive and sense ports (indicated as D+, D-, S+, S- in the figure) are sent to a pair of band-pass filters, so to avoid noise folding in the following saturation stage from sine to square wave [10, 11]. This procedure optimizes resolution in the following phase measurement (Fig. 2b-c) performed by an off-the-shelf frequency meter. On the printed circuit board, all passive components (even if outside the chamber) are chosen with ultra-high temperature stability to avoid small undesired drifts during long-term acquisitions where the board remains in uncontrolled laboratory environment.

In a preliminary setup calibration on a single MEMS, an open-loop spectral characterization that forces the drive axis while reading the sense output is repeated twice (rotor voltage on/off) to quantify the parasitic coupling coefficients (amplitude and phase). The measurements results are shown in Fig. 3. The estimated value can be then multiplied by the drive signal (itself a function of the quality factor, thus of T) and subtracted for every MEMS phase, at every temperature, as all the electronics remains outside the chamber.

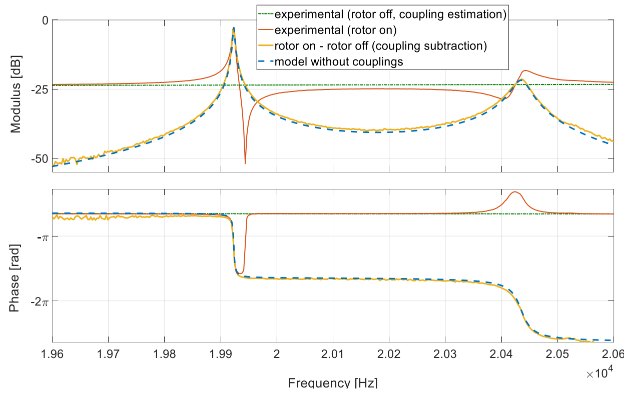

Fig. 3: modulus/phase calibration of parasitic couplings. Curves refer to a MEMS with 650 dps quadrature, but the setup calibration remains valid for all other experiments.

To characterize achievable relative phase resolutions, short-term and long-term measurements were processed through the Allan variance method. Fig. 4 shows how no drift is observed on short-term phase measurements (typically captured at every °C-step during temperature sweeps), and how white phase noise remains lower than 2 μrad/√Hz. On a longer term (just one thick measurement shown), 1/f phase noise becomes visible with a stability in the order of 3 μrad for observation intervals as large as 100 s (1000 s overall measurement time). These results essentially meet the specification discussed in the introduction.

III. RESULTS

The experimental campaign to evaluate the phase drift as a function of temperature was performed on four different samples characterized by native, uncompensated quadrature values in the range between about 600 dps and about 12000 dps. The gyroscopes can be actuated at different drive amplitudes by acting on the voltage V_{ref} in the amplitude control loop of Fig. 2. Their mode-split value can be changed by changing the rotor voltage (this in turns partially affects also achievable phase noise, [12]).

Fig. 5 reports sample measured curves of the uncompensated phase drift of one device in four testing conditions at different rotor voltages and identical drive amplitude, to validate the drift slope changes as a function of the drive signal amplitude, for the same, calibrated, coupling

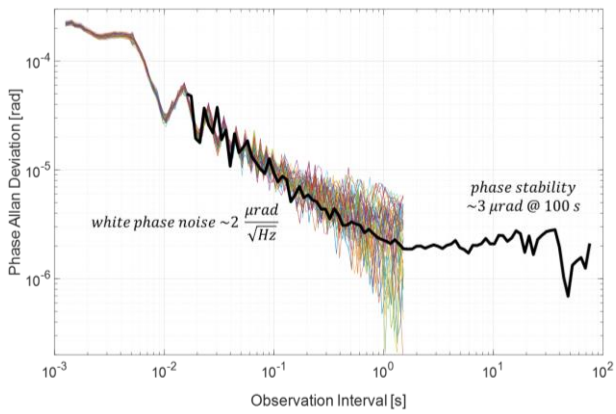

Fig. 4: Allan deviation of 45 phase acquisitions captured during temperature sweeps at 1°C difference each, and single long-term acquisition (thick curve) showing 2-μrad/√Hz noise density and 3-μrad stability.

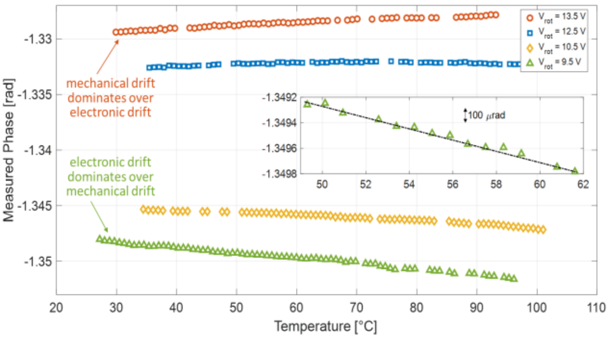

Fig. 5: measured phase vs T in various testing conditions. As expected, at larger rotor voltages, for the same drive motion of 6.5 µm, AC drive signals are lower and effects of electronic couplings decrease, leaving the mechanical drift evident. The inset shows a phase measurement accuracy in the 10-µrad range during long-term (8 hours) acquisitions.

coefficient. What happens is essentially that, for the same target motion amplitude, a reduction of the rotor voltage requires a larger drive amplitude, which induces larger parasitic couplings and in turn a more visible electronic drift (negative slope in the curves). When the rotor voltage is increased, on the contrary, the drive voltage amplitude and its couplings are reduced, leaving the mechanical drift term dominant (positive slopes in Fig. 5).

Finally, Fig. 6 isolates the mechanical phase drift (1st-order coefficient), reported on the y-axis as a function of the different samples in various conditions (reported along the x-axis). In particular, the drive amplitude varies from 2.4 µm to a maximum value of 6.5 µm, while the rotor voltage is swept from a minimum of 9 V (about 700-Hz split) to a maximum of 13.5 V (about 200-Hz split). The dashed curve refers to the model without corrections for electronic drifts, the solid curve includes such corrections, and the red square markers represent the measured data.

Not only an almost perfect agreement is obtained (12 µrad/K rms deviation from the model), especially at large quadrature values, but such a capability to precisely measure the phase vs temperature enables identifying deviations from the model, in light of a possible ultra-accurate online compensation of offset drifts.

IV. Conclusions and Future Work

The work proposed a thorough analysis of the temperature drift of the relative phase between the Coriolis signal and the drive demodulation reference in capacitive amplitude-modulated gyroscopes, which is a fundamental effect in determining their ultimate rate stability.

After evaluating the specifications in terms of required phase noise and phase stability, dedicated instrumentation was developed reaching 2 µrad/√Hz resolution without noticeable drifts after 100 s, and good agreement with phase-drift model prediction based on the *TCf* and *TCQ*.

The experimental measurement campaign was performed on several samples and in various conditions, but on a single device type so far. In the near future, plans are to test the instrument with other gyroscope types and to extend the model so to identify other effects like the drift of the quadrature itself.

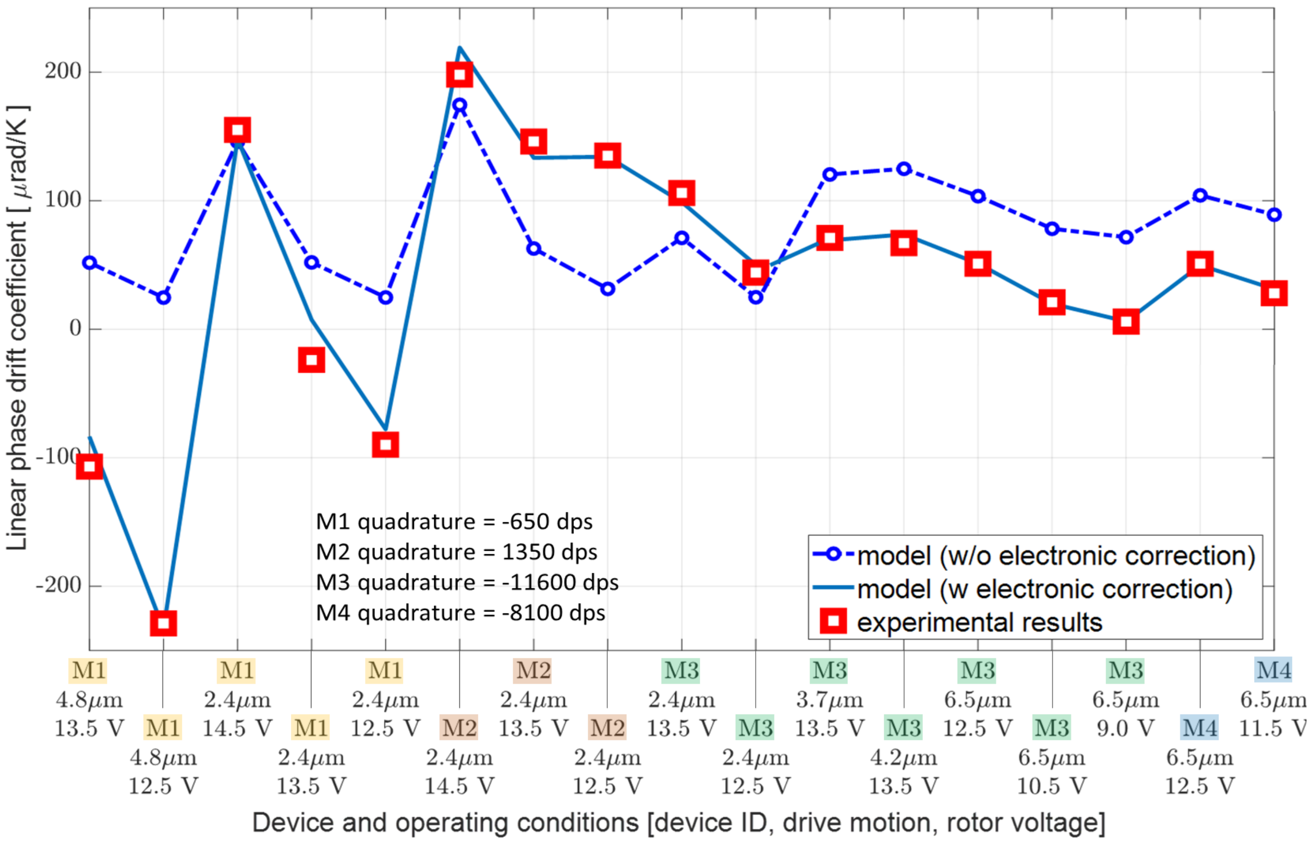

Fig. 6: once electronic coupling coefficients are found through the initial calibration of Fig. 3, the measurements match (within 12 µrad/K) the predicted phase drift for different combinations of split values (rotor voltage), drive amplitude (AGC voltage V_{REF}) and quadrature (device ID).

References

[1] E. Tatar, S. E. Alper and T. Akin, "Quadrature-Error Compensation and Corresponding Effects on the Performance of Fully Decoupled MEMS Gyroscopes," in *Journal of Microelectromechanical Systems*, vol. 21, no. 3, pp. 656-667, June 2012.

[2] S. Facchinetti, L. Guerinoni, L. G. Falorni, A. Donadel and C. Valzasina, "Development of a complete model to evaluate the Zero Rate Level drift over temperature in MEMS Coriolis Vibrating Gyroscopes," *2017 IEEE International Symposium on Inertial Sensors and Systems (INERTIAL)*, Kauai, HI, 2017, pp. 125-128.

[3] C. D. Ezekwe, W. Geiger and T. Ohms, "27.3 A 3-axis open-loop gyroscope with demodulation phase error correction," *2015 IEEE International Solid-State Circuits Conference - (ISSCC) Digest of Technical Papers*, San Francisco, CA, 2015, pp. 1-3.

[4] G. K. Balachandran, V. P. Petkov, T. Mayer and T. Balslink, "A 3-Axis Gyroscope for Electronic Stability Control With Continuous Self-Test," in *IEEE Journal of Solid-State Circuits*, vol. 51, no. 1, pp. 177-186, Jan. 2016.

[5] G. Langfelder, C. Buffa, A. Frangi, A. Tocchio, E. Lasalandra and A. Longoni, "Z-Axis Magnetometers for MEMS Inertial Measurement Units Using an Industrial Process," in *IEEE Transactions on Industrial Electronics*, vol. 60, no. 9, pp. 3983-3990, Sept. 2013.

[6] G. Mussi, M. Bestetti, V. Zega, A. Frangi, G. Gattere and G. Langfelder, "Resonators for real-time clocks based on epitaxial polysilicon process: A feasibility study on system-level compensation of temperature drifts," *2018 IEEE Micro Electro Mechanical Systems (MEMS)*, Belfast, 2018, pp. 711-714.

[7] B. Kim *et al*., "Temperature Dependence of Quality Factor in MEMS Resonators," in *Journal of Microelectromechanical Systems*, vol. 17, no. 3, pp. 755-766, June 2008.

[8] L. Gaffuri Pagani, S. Dellea, G. Bursi, M. Brunetto, L. Falorni and G. Langfelder, "Enhancing Vibration Robustness and Noise in Automotive Gyroscope with Large Drive Motion and Levered Sense Mode," *2019 IEEE 32nd International Conference on Micro Electro Mechanical Systems (MEMS)*, Seoul, Korea (South), 2019, pp. 708-711.

[9] L. Prandi *et al*., "A low-power 3-axis digital-output MEMS gyroscope with single drive and multiplexed angular rate readout," *2011 IEEE International Solid-State Circuits Conference*, San Francisco, CA, 2011, pp. 104-106.

[10] M. Pardo, L. Sorenson and F. Ayazi, "An Empirical Phase-Noise Model for MEMS Oscillators Operating in Nonlinear Regime," in *IEEE Transactions on Circuits and Systems I: Regular Papers*, vol. 59, no. 5, pp. 979-988, May 2012.

[11] C. R. Marra *et al*., "Optimization of low-power oscillator topology for frequency modulated MEMS inertial sensors," *2018 European Frequency and Time Forum (EFTF)*, Turin, 2018, pp. 122-125.

[12] D. K. Agrawal and A. A. Seshia, "An analytical formulation for phase noise in MEMS oscillators," in *IEEE Transactions on Ultrasonics, Ferroelectrics, and Frequency Control*, vol. 61, no. 12, pp. 1938-1952, Dec. 2014.